Effect of the Prosthetic Group on the Pharmacologic Properties of ^{18}F-Labeled Rhodamine B, a Potential Myocardial Perfusion Agent for Positron Emission Tomography (PET)

Mark D. Bartholomä,[†,‡,§] Vijay Gottumukkala,[†,‡] Shaohui Zhang,[†,‡] Amanda Baker,[†] Patricia Dunning,[†] Frederic H. Fahey,[†,‡] S. Ted Treves,[†,‡] and Alan B. Packard*,[†,‡]

[†]Division of Nuclear Medicine and Molecular Imaging, Boston Children's Hospital, Boston, Massachusetts 02115, United States
[‡]Harvard Medical School, Boston, Massachusetts 02115, United States

Ⓢ *Supporting Information*

ABSTRACT: We recently reported the development of the 2-[^{18}F]fluoroethyl ester of rhodamine B as a potential positron emission tomography (PET) tracer for myocardial perfusion imaging. This compound, which was prepared using a [^{18}F]fluoroethyl prosthetic group, has significant uptake in the myocardium in rats but also demonstrates relatively high liver uptake and is rapidly hydrolyzed in vivo in mice. We have now prepared ^{18}F-labeled rhodamine B using three additional prosthetic groups (propyl, diethylene glycol, and triethylene glycol) and found that the prosthetic group has a significant effect on the in vitro and in vivo properties of these compounds. Of the esters prepared to date, the diethylene glycol ester is superior in terms of in vitro stability and pharmacokinetics. These observations suggest that the prosthetic group plays a significant role in determining the pharmacological properties of ^{18}F-labeled compounds. They also support the value of continued investigation of ^{18}F-labeled rhodamines as PET radiopharmaceuticals for myocardial perfusion imaging.
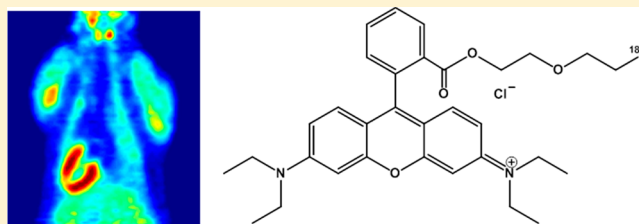
INTRODUCTION

Cardiovascular disease is a major health problem worldwide, and noninvasive imaging modalities such as single-photon emission computed tomography (SPECT) and positron emission tomography (PET) play a key role in the diagnosis and treatment planning for this disease. The limitations of single-photon tracers, including the absence of a standardized attenuation correction method, which can result in attenuation artifacts in obese patients or women with large or dense breast tissue, the inability to perform quantitative measurements, which are useful for the detection of balanced ischemia, the higher spatial resolution and sensitivity of PET, and recurring shortages of ^{99m}Tc, all argue for an increased role for PET in myocardial perfusion imaging (MPI).[1,2]

Despite its advantages, the tracers that are currently available for PET MPI suffer from significant practical limitations. The short half-lives of [15]O (2 min) and [13]N (10 min) limit their use to clinical centers with an on-site cyclotron. Rubidium-82 ($t_{1/2}$ = 76 s) is generator produced, allowing its use at clinics without access to cyclotrons, but the high cost of the generator limits its use to facilities with high patient throughput. Other limitations of [82]Rb include less than optimal myocardial extraction and high positron energy, which decreases spatial resolution.[1] These limitations have spurred interest in the development of ^{18}F-labeled myocardial perfusion tracers.[3,4]

The physical properties of [18]F (β^+, 0.635 MeV [97%]; $t_{1/2}$ = 110 min) are nearly ideal for PET, and distribution networks have already been established for [^{18}F]2-fluorodeoxyglucose ([^{18}F]FDG), demonstrating that production of ^{18}F-labeled radiopharmaceuticals at central sites is a reasonable alternative to on-site production. An additional advantage of the 110 min half-life is that while it is long enough to allow distribution from central production facilities, it is still short enough to allow repeated (rest/stress) MPI studies of a patient on the same day. Repeated single-day MPI studies are routinely performed using ^{99m}Tc MPI radiopharmaceuticals ($t_{1/2}$ = 6 h),[5] and recently, the applicability of ^{18}F MPI radiopharmaceuticals for single-day MPI studies was demonstrated for flurpiridaz F 18.[6,7]

Several ^{18}F-labeled compounds have been proposed as possible MPI radiopharmaceuticals including quaternary ammonium salts,[8] tetraphenylphosphonium compounds,[9−12] rotenone derivatives,[13,14] and pyridazinone analogues, such as BMS-747158-02 (flurpiridaz F 18, Lantheus Medical Imaging).[15−21] Of these compounds, flurpiridaz has been the subject of the most extensive evaluation to date.[6,22,23]

Like the single-photon MPI tracers ^{99m}Tc-methoxyisobutylisonitrile (^{99m}Tc-MIBI) and ^{99m}Tc-tetrofosmin and the ^{18}F-labeled tetraphenylphosphonium derivatives, rhodamine B is a lipophilic cation (Figure 1). Other properties that rhodamine B shares with ^{99m}Tc-MIBI and ^{99m}Tc-tetrofosmin include localization in mitochondria[24−27] and being a substrate for P-
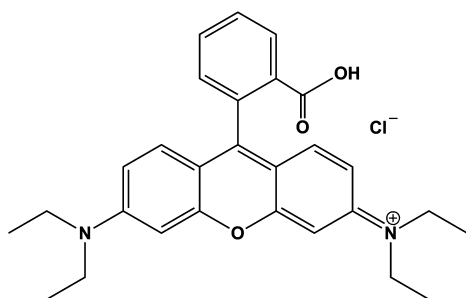
Figure 1. Rhodamine B.

glycoprotein, which is involved in multidrug resistance.[28,29] Furthermore, it was found that nonradiolabeled rhodamine 123 accumulates in mouse heart.[30] These properties suggested that [18F]-labeled rhodamines are promising candidates for evaluation as potential PET MPI radiopharmaceuticals.

We recently described the synthesis and initial biological evaluation of an [18F]-labeled rhodamine B ester, 2-[[18F]-fluoroethyl rhodamine B ([18F]3, Figure 2), as a potential PET radiopharmaceutical for the evaluation of myocardial perfusion.[31,32] In these studies, we found that although [18F]3 did not accumulate in mouse myocardium, presumably because of rapid in vivo hydrolysis of the 2-fluoroethylester prosthetic group, it did demonstrate significant uptake in the rat heart. The pharmacologic properties of [18F]3 are, however, less than optimal, particularly with respect to uptake and clearance from the liver.

Prosthetic groups are a convenient way to radiolabel organic species containing secondary amine or carboxylate moieties with [18F],[33−36] and by far the most commonly used prosthetic group, particularly with respect to carboxylates, is 2-fluoroethyl, which was used to prepare [18F]3. Henrikson and co-workers measured the in vivo stability of the [18F]-labeled methyl and ethyl esters of carfentanil in mice and found that only 2% of the methyl ester remained intact in the serum at 40 min after injection while 5−6% of the ethyl ester remained intact at 40 min.[37] Erlandsson and co-workers measured the stability of the [18F]-labeled ethyl esters of the 4-chloro- and 4-bromometomidate in rats[38] and found that that only 6% of the chloro compound remained intact 30 min after injection while 39% of the bromo compound remained intact at the same time point. These investigators also measured the metabolic stability of the diethylene and triethylene glycol esters of metomidate in rats

and found that only 2% of the diethylene glycol ester remained intact at 30 min after injection compared to 6% of the triethylene glycol ester.[39] In combination, these results suggest, somewhat unexpectedly, that changing the ester group has minimal impact on the in vivo stability of these compounds.

Given the popularity of 2-fluoroethyl as a prosthetic group, particularly in the preparation of [18F]-labeled esters, and the propensity of carboxylic esters to undergo in vivo hydrolysis, especially in mice,[40] it is somewhat surprising that there has not been a more extensive evaluation of alternative prosthetic groups that might be more resistant to in vivo degradation. Here, we report our recent efforts to address this issue while at the same time improving the pharmacologic properties of [18F]-labeled rhodamine B by evaluating the effect of changing the prosthetic group on the biodistribution and serum stability of the corresponding rhodamine B esters.

■ RESULTS AND DISCUSSION

In previous studies, we demonstrated the feasibility of using [18F]3 as a myocardial perfusion agent in rats.[32] The liver uptake of this compound was, however, less than optimal and interfered with the visualization of the myocardium. In the present study, we evaluated three alternative prosthetic groups to determine if, by changing the prosthetic group, we could decrease the concentration of the compound in the liver and/or increase the rate of clearance from the liver while simultaneously maintaining or increasing tracer accumulation in the heart.

Synthesis of [18F]-Labeled Rhodamine B Esters. The three tracers ([18F]4, propyl ester; [18F]5, diethylene glycol ester; [18F]6, triethyleneglycol ester) were prepared in good yield and high radiochemical purity using the one-pot reaction (Figure 2) previously used to prepare [18F]3 followed by purification by semipreparative high performance liquid chromatography (HPLC).[31,32] The identity of the tracers was confirmed by analytical HPLC using the nonradioactive ([19F]) compounds as reference materials.

The total synthesis time was 120 min, and the desired products were obtained in >97% radiochemical purity in decay-corrected yields of 18 ± 1%, 19 ± 1%, and 22 ± 3% for [18F]4, [18F]5, and [18F]6, respectively. The specific activities of [18F]4, [18F]5, and [18F]6 are 50, 310, and 320 MBq/μmol (1.35, 8.38, and 8.65 mCi/μmol), respectively (Table 1). The low specific activities are a consequence of the formation of byproducts in the reaction of the ditosyl precursor with
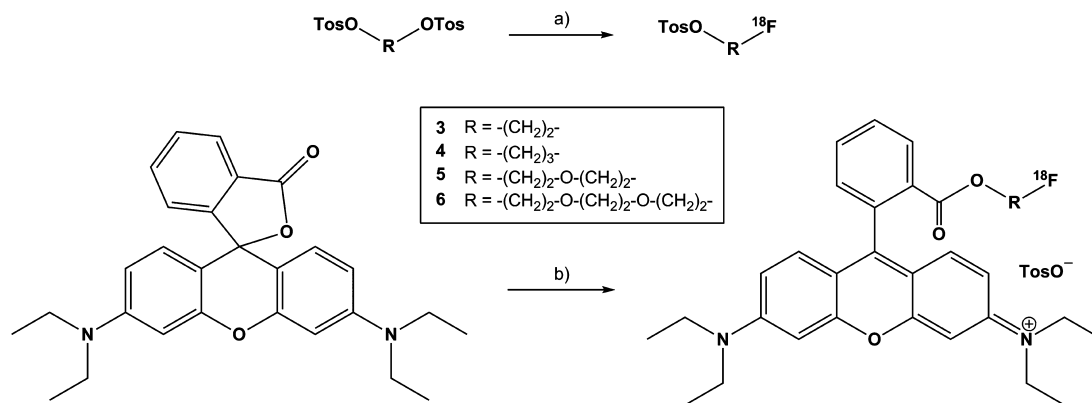

Figure 2. Radiosyntheses of the previously described ethyl ester [18F]3 and the new compounds [18F]4, [18F]5, and [18F]6: (a) K$_2$CO$_3$/K2.2.2, ACN, 90 °C, 10 min; (b) DIPEA, ACN, 165 °C, 30 min.

Table 1. In Vitro Stability, Partition Coefficients and Specific Activities for the Three Rhodamine B Derivatives

compd	serum stability[a] (%)	log P	specific activity
[18F]4	99.6 ± 0.7[b]	2.15 ± 0.01	50 MBq/μmol (1.4 mCi/μmol)
	96.1 ± 0.8[c]		
	99.0 ± 0.4[d]		
[18F]5	97.1 ± 1.6[b]	1.90 ± 0.01	310 MBq/μmol (8.4 mCi/μmol)
	96.1 ± 2.0[c]		
	97.1 ± 1.1[d]		
[18F]6	92.1 ± 1.2[b,e]	1.99 ± 0.01	320 MBq/μmol (8.6 mCi/μmol)
	87.2 ± 1.4[c,e]		
	97.2 ± 1.1[d,e]		

[a]At 120 min unless otherwise stated. [b]Mouse serum. [c]Rat serum. [d]Human serum. [e]At 15 min.

rhodamine B (i.e., 2-(2-tosylethoxy)ethyl rhodamine B and 2-(2-hydroxyethoxy)ethyl rhodamine B, formed by in situ hydrolysis of 2-(2-tosylethoxy)ethyl rhodamine B for [18F]5). Because of the chemical similarity to the 18F-labeled product, the only difference being a terminal -F vs -OH or -Tos group, these byproducts are not separated in the final semipreparative HPLC purification. We have recently shown for [18F]3 that HPLC purification of the 18F-labeled tosyl precursor prior to the reaction with rhodamine B lactone results in higher specific activities.[32] However, the additional HPLC purification of the

precursor significantly increases the overall synthesis time and thus significantly lowers the overall radiochemical yield. Since the low specific activities did not interfere with the characterization of the tracers, the additional HPLC purification step was omitted in favor of increased radiochemical yield at the developmental stage. Nonetheless, efforts to further increase the specific activity of 18F-labeled rhodamine are currently underway.

The partition coefficients of [18F]4, [18F]5, and [18F]6 are also summarized in Table 1.

Synthesis of Nonradioactive (19F) Compounds. The nonradioactive 19F derivatives **4**, **5**, and **6** were prepared as reference materials for the HPLC characterization of the 18F compounds and for determination of the specific activity. The corresponding NMR spectra and mass spectrometry data are provided in Supporting Information (Figures S1−S11). Compound **4** was obtained in 73% yield by reacting rhodamine B chloride salt with commercially available 3-fluoropropan-1-ol using the coupling reagents N-hydroxysuccinimide (NHS) and N,N′-dicyclohexylcarbodiimide (DCC). Purification of the crude reaction mixture by conventional silica gel column chromatography was not successful; therefore, the product was purified by semipreparative HPLC. In contrast, compounds **5** and **6** were prepared similarly to the 18F compounds, by reacting rhodamine B lactone with the corresponding fluoroethylene glycol esters **1** and **2**, respectively. Precursors **1** and **2** were prepared in good yield (74−83%) from the corresponding ditosylates and 1 M tetrabutylammonium fluoride (TBAF) in
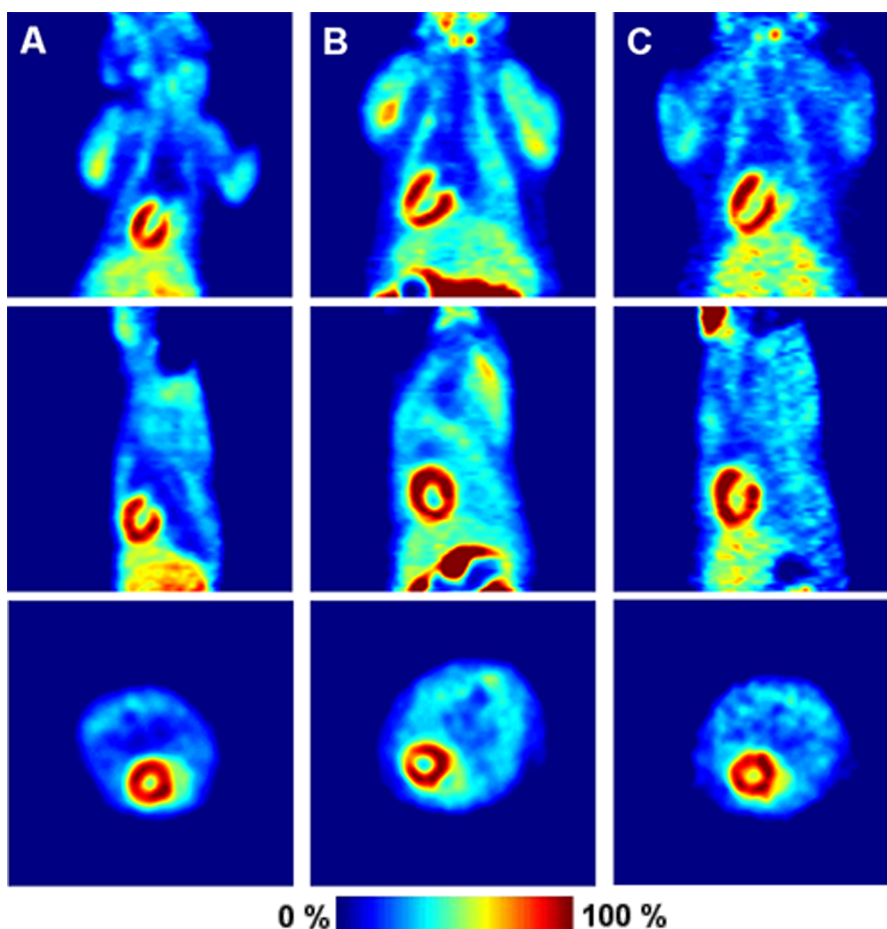

Figure 3. Coronal (top), sagittal (middle), and transverse (bottom) microPET images of [18F]4 (A), [18F]5 (B), and [18F]6 (C) in the rat.
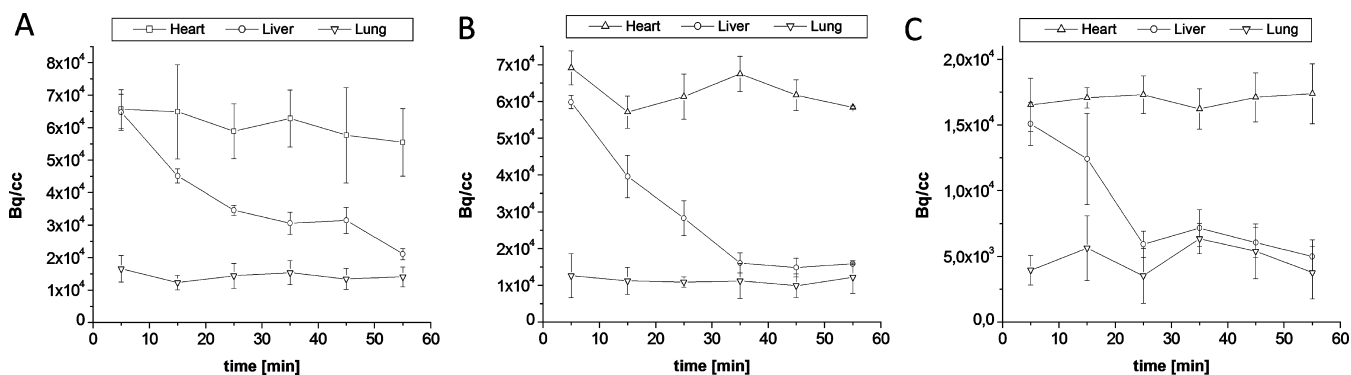
Figure 4. Time−activity curves (TACs) of the heart, liver, and lung constructed from microPET images of $[^{18}F]4$ (A), $[^{18}F]5$ (B), and $[^{18}F]6$ (C) in the rat.

tetrahydrofuran (THF) with minor modifications to a procedure described by Mavel et al.[41] Reaction of the precursors with rhodamine B lactone in the presence of diisopropylethylamine (DIPEA) gave **5** and **6** in 26% and 29% yield after HPLC purification. All reference compounds were characterized by proton and fluorine NMR spectroscopy and mass spectrometry.

Serum Stability Studies. The stability of $[^{18}F]4$, $[^{18}F]5$, and $[^{18}F]6$ was measured in vitro at 37 °C in mouse, rat, and human serum and in phosphate buffered saline (PBS) at 15, 30, 60, and 120 min. As expected, no degradation was observed for any of the compounds in PBS for up to 2 h of incubation time. The 3-$[^{18}F]$fluoropropyl ester, $[^{18}F]4$, remained >95% intact for 2 h in all tested sera (Supporting Information Figure S14), and a similar result was obtained for $[^{18}F]5$ with 97% of the compound present after 2 h (Supporting Information Figure S15). These results are substantially different from those obtained for $[^{18}F]3$, which was rapidly degraded in mouse serum with only 25% of the compound being intact after 2 h of incubation time.

For $[^{18}F]6$, a rather unusual degradation pattern was noted. In all tested sera, up to 10% decomposition was observed after the initial 15 min, but no further degradation occurred at later time points (Supporting Information Figure S16). Further degradation was, however, observed upon the addition of fresh serum to the mixture. This pattern is different from that observed for $[^{18}F]3$, which decomposed continuously over the 2 h time period of the study. One possible explanation for this effect would be that the compound responsible for the degradation of the triethylene glycol ester is present in limited amounts in all tested sera. If this is the case, this would probably result in a more extensive degradation in vivo as the blood-to-tracer ratio would be much higher and the protein responsible for the degradation would not be depleted as quickly. This phenomenon does not, however, negatively impact the ability of this compound to accumulate in the heart, as $[^{18}F]6$ shows high and persistent uptake in the myocardium (vide infra).

The increased stability of $[^{18}F]4$, $[^{18}F]5$, and $[^{18}F]6$ compared to the previously reported compound ($[^{18}F]3$) is presumably a consequence of the increasing basicity of the corresponding fluoroalkyl prosthetic groups. For example, it was found for benzoate esters that the rate of ester hydrolysis decreases with increasing basicity (decreasing acidity) of the alkyl leaving group.[42] Furthermore, the acidity of alkyl alcohols (e.g., methanol, ethanol, and *n*-propanol) decreases with increasing alkyl chain length as exemplified by the corresponding pK_a values.[43,44] Additionally, an electron withdrawing

substituent, such as a fluorine atom or a methoxy group, decreases the basicity of the corresponding alcohols (e.g., F-CH_2-CH_2-OH ∼ CH_3-O-CH_2-CH_2-OH < CH_3-CH_2-OH).[43] As the propyl, diethylene glycol, and triethylene glycol rhodamine esters are more stable than the ethyl ester, a similar trend may be true for ^{18}F-labeled rhodamines.

Small-Animal PET Imaging. Representative 60 min (summed) small-animal PET images obtained with $[^{18}F]4$, $[^{18}F]5$, and $[^{18}F]6$ in rats are shown in Figure 3.

These PET images clearly show high and persistent retention in the myocardium and high contrast between the myocardium and blood, liver, bone, and lungs for all three compounds. In all cases, including $[^{18}F]6$ (Figure 3C), which showed greater decomposition in rat serum than $[^{18}F]4$ and $[^{18}F]5$, the heart is much more clearly defined than with $[^{18}F]3$. For all three compounds, the liver uptake is significantly lower than that of $[^{18}F]3$, with $[^{18}F]4$ and $[^{18}F]6$ being similar to each other and $[^{18}F]5$ being somewhat lower than $[^{18}F]4$ and $[^{18}F]6$. In all three cases there is excretion of tracer through the gut and the kidneys. A representative maximum intensity projection video showing the distribution of $[^{18}F]5$ is available as Supporting Information.

The microPET images also reveal high accumulation of each tracer in the neck, as was observed for $[^{18}F]3$, possibly representing the parathyroid or salivary gland accumulation, and in the muscles of the forelimbs. The bone uptake in all cases is minimal, with the skeleton being barely visible, suggesting minimal in vivo defluorination.

Time−activity curves of $[^{18}F]4$, $[^{18}F]5$, and $[^{18}F]6$, shown in Figure 4, reveal rapid liver clearance and no significant washout from the myocardium over the 60 min imaging period. Of the three new compounds, the initial liver concentration of $[^{18}F]5$ is lower and the liver clearance is faster compared to $[^{18}F]4$ and $[^{18}F]6$. Thus, for $[^{18}F]5$, the heart concentration (69 ± 5 kBq/cm³) at 5 min post injection (pi) is somewhat higher than that in the liver (59 ± 2 kBq/cm³) while for $[^{18}F]4$ (66 ± 6 kBq/cm³ vs 65 ± 6 kBq/cm³) and $[^{18}F]6$ (16 ± 2 kBq/cm³ vs 15 ± 2 kBq/cm³) the concentrations are essentially equal. At 35 min pi, the heart-to-liver ratio for $[^{18}F]5$ increases to 4.2 while the heart-to-liver ratios for $[^{18}F]4$ and $[^{18}F]6$ increase to 2.0 and 2.3, respectively. These differences can also be seen in a comparison of the clearance rates of the tracers from the liver. At 55 min pi, the liver concentration of $[^{18}F]5$ is 25% of the 5 min value while the corresponding values for $[^{18}F]4$ and $[^{18}F]6$ are in the range 30−35%.

These observations are in agreement with the microPET images (Figure 3), which show that the heart is much more
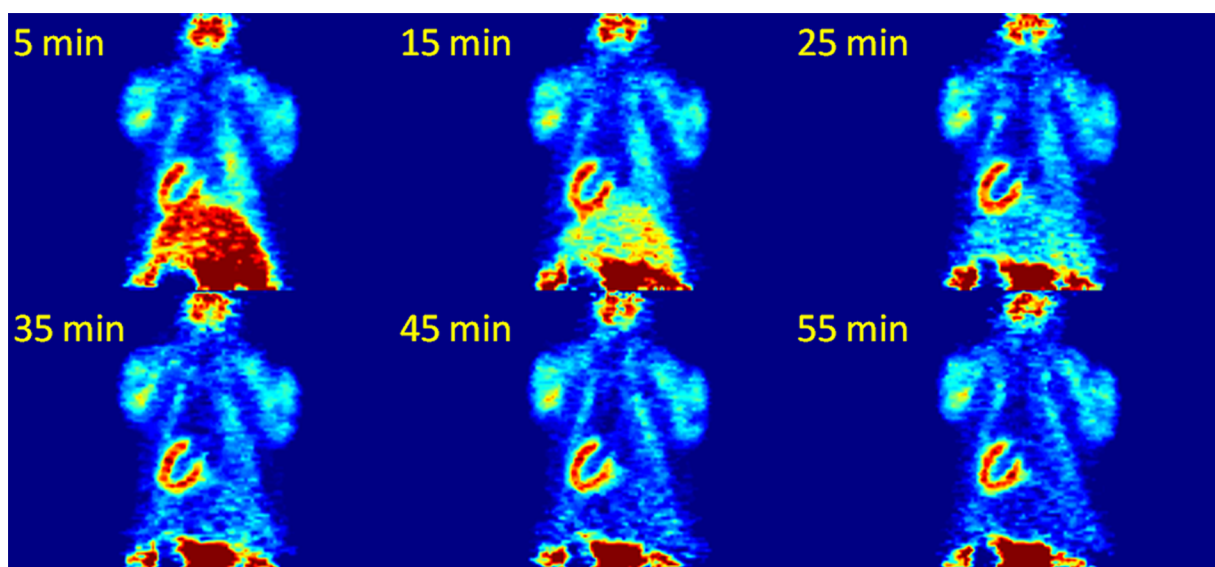
Figure 5. Time-resolved microPET image of compound [¹⁸F]5 in the rat showing persistent retention in the heart and clearance of [¹⁸F]5 from the liver.

Table 2. Rat Biodistribution Data for the Four Rhodamine B Esters at 60 min pi[a]

	compd			
tissue	[¹⁸F]3[b]	[¹⁸F]4	[¹⁸F]5	[¹⁸F]6
blood	0.08 ± 0.03	0.05 ± 0.01	0.25 ± 0.02	0.19 ± 0.01
heart	2.06 ± 0.61	1.32 ± 0.13	2.51 ± 0.16	1.03 ± 0.13
lung	1.78 ± 0.65	1.58 ± 0.19	2.06 ± 0.16	0.56 ± 0.05
liver	0.89 ± 0.07	0.55 ± 0.11	0.49 ± 0.04	0.25 ± 0.03
spleen	5.63 ± 0.78	3.82 ± 0.32	3.53 ± 0.57	0.83 ± 0.10
kidney	8.31 ± 0.81	8.26 ± 1.62	9.28 ± 0.66	3.24 ± 0.43
gut	2.40 ± 0.53	2.53 ± 0.67	1.69 ± 0.42	0.44 ± 0.09
skin	0.20 ± 0.02	0.20 ± 0.07	0.36 ± 0.04	0.24 ± 0.03
muscle	0.16 ± 0.04	0.30 ± 0.01	0.54 ± 0.07	0.32 ± 0.05
bone	0.45 ± 0.08	0.65 ± 0.08	0.77 ± 0.04	0.38 ± 0.07
heart/blood[c]	25.8	26.4	10.0	5.4
heart/lung[c]	1.6	0.8	1.2	1.8
heart/liver[c]	2.3	2.4	5.1	4.1
heart/bone[c]	4.6	2.0	3.3	2.7

[a]Results are expressed as the mean %ID/g ± ESD for $n = 5$. [b]Reference 32. [c]Tissue ratios.

clearly defined with the diethylene glycol ester, [¹⁸F]5, compared to the other esters.

Figure 5 shows the six 10-min frames for compound [¹⁸F]5 from which the time−activity curves (TACs) were derived. This series of images shows that [¹⁸F]5 is essentially cleared from the liver after 30 min, while the tracer is retained in the myocardium through the 60 min scan.

Small-animal PET images were also obtained for [¹⁸F]5 and [¹⁸F]6 in mice to determine if the observed increase in in vitro stability translated into improved myocardial uptake (Supporting Information, Figures S12 and S13). While both compounds showed appreciable uptake in the myocardium, there was also significant uptake in the kidneys, spleen, gall bladder, and subsequently the intestine. This pattern of uptake, particularly the high uptake in the gall bladder, suggests that while these compounds are more stable in mice than [¹⁸F]3, they are not stable enough to justify using mice for subsequent studies.

Biodistribution Studies. The results of the 60 min biodistribution studies in rats carried out for [¹⁸F]4, [¹⁸F]5, and [¹⁸F]6 are summarized in Table 2.

Of the three compounds in the present study, the highest heart concentration is observed for [¹⁸F]5 (2.51 ± 0.16% injected dose/gram) (%ID/g) followed by [¹⁸F]6 (1.32 ± 0.13 %ID/g) and [¹⁸F]4 (1.03 ± 0.13 %ID/g). The heart concentration of [¹⁸F]5 is somewhat higher than that of the previously described ethyl ester, [¹⁸F]3 (2.06 ± 0.61 %ID/g), but the difference is not statistically significant. The heart concentration of [¹⁸F]5 is, however, significantly greater than those of [¹⁸F]4 and [¹⁸F]6 ($P < 0.0001$). The liver concentration of [¹⁸F]5 at 60 min pi (0.49 ± 0.04 %ID/g) is significantly lower than that of [¹⁸F]3 (0.89 ± 0.07 %ID/g, $P < 0.0001$), higher than that of [¹⁸F]6 (0.25 ± 0.03 %ID/g, $P < 0.0001$), and essentially equal to that of [¹⁸F]4 (0.55 ± 0.11 %ID/g). These increases in tracer uptake by the heart and decreases in uptake by the liver for [¹⁸F]5 and [¹⁸F]6 lead to significant improvements in the heart-to-liver ratios for these compounds compared to the prototype compound. The heart-to-liver ratio for [¹⁸F]3 was 2.3 while the ratios for [¹⁸F]5 and [¹⁸F]6 are 5.1 and 4.1, respectively, suggesting that [¹⁸F]5 is the preferred compound.

The blood activity for all three tracers is very low at 60 min after injection (<0.25 %ID/g). The heart-to-blood ratios for [18F]**4**, [18F]**5**, and [18F] **6** are 26.4, 10.0, and 5.4, respectively. The bone concentration for all three tracers is less than 1 %ID/g, consistent with minimal in vivo defluorination. There is significant accumulation of each tracer in the kidney and gut, suggesting a combination of renal and hepatobiliary excretion. There is also significant accumulation of all three tracers in the lungs and the spleen. This may be due to aggregation, as the apparent specific activity of these compounds is relatively low (Table 1) and rhodamines are known to aggregate even at submicromolar concentrations.[45] Efforts are currently underway to increase the specific activity of the compound, which, if this hypothesis is correct, will reduce tracer uptake in these nontarget organs. It is, however, important to note that this does not interfere with visualization of the heart.

The results of the biodistribution studies of [18F]**4**, [18F]**5**, and [18F]**6** may also be compared to other 18F-labeled myocardial perfusion tracers currently under development. There are several reports of biodistribution studies in rats of flurpiridaz, an 18F-labeled MPI agent that is currently in late-stage clinical trials. In Wistar rats, this compound exhibited heart uptake of 2.06 %ID/g at 60 min pi, a result that is somewhat lower than the uptake of [18F]**5** (2.51 %ID/g).[16] In Sprague–Dawley rats, however, flurpiridaz F 18 showed heart uptake with 3.3 %ID/g at 60 min pi.[17,46] In the Wistar rat study, flurpiridaz F 18 cleared quickly from the liver (0.99 %ID/g at 10 min pi vs 0.38 %ID/g at 60 min pi), the 60 min value being somewhat lower than that observed for [18F]**5** (0.49 %ID/g).[16]

As noted above, the heart-to-liver ratio is of particular importance for a myocardial perfusion tracer. The heart-to-liver ratio for [18F]**5** at 60 min pi (5.1) is similar to that of flurpiridaz F 18, 5.4 in Wistar rats and 3.7 in Sprague–Dawley rats,[16,46] and the heart-to-blood ratio of flurpiridaz F 18 at 60 min pi (13.7) is slightly higher than that of [18F]**5** (10.0).[13]

Another 18F-labeled myocardial perfusion tracer currently in clinical trials is 4-[18F]fluorophenyl)triphenylphosphonium (18F-FTPP), an 18F-labeled analogue of the tetraphenylphosphonium cation.[12] This compound exhibits heart uptake of 1.64 %ID/g at 5 min, 1.51 %ID/g at 30 min, and 1.57 %ID/g at 60 min pi in Sprague–Dawley rats.[12] At 60 min pi, the liver concentration of 18F-FTPP is 0.17 %ID/g, significantly lower than that of [18F]**5** (0.48 %ID/g) and flurpiridaz F 18 (0.38 % ID/g). Thus, at 60 min pi, the heart-to-liver ratio of 18F-FTPP is 9.2 compared to 5.1 for [18F]**5** and 5.4 for flurpiridaz F 18. Fluorine-18-FTPP is rapidly cleared from blood with the heart-to-blood ratio increasing from 11 at 5 min to 75 at 60 min pi.

As previously noted, it is well-known that ethyl esters are susceptible to rapid hydrolysis in mouse serum,[47] and it appears likely that the three esters in the present study (propyl, diethylene glycol, and triethylene glycol) undergo a similar decomposition process, albeit to a different extent depending on the ester moiety. Irrespective of the mechanism, the rate of decomposition of the three new compounds is apparently slow enough to allow accumulation of the tracers in the heart, in contrast to the results observed for the ethyl ester. The net result is that using diethylene glycol as the prosthetic group results in higher in vitro stability and significantly improves the pharmacokinetics of 18F-labeled rhodamines. In this context, it is worth noting that this is one of the few examples where diethylene glycol (or triethylene glycol) has been used as a prosthetic group for labeling a compound with 18F.

These results are somewhat disparate from those obtained by Erlandsson et al. in their studies of ethyl esters of chloro- and bromometomidate and of the of the triethylene and diethylene glycol esters of metomidate.[38,39] These investigators found that the ethyl ester was slightly more stable in vivo than the diethylene glycol ester and that the difference between stability of the triethylene and diethylene glycol esters was minimal.

CONCLUSIONS

On the basis of the promising initial results with [18F]**3**, we expanded our efforts to develop a myocardial perfusion tracer based on 18F-labeled rhodamines. The focus of the current effort was to improve the stability and pharmacokinetics compared to the original compound. Therefore, we evaluated different prosthetic groups: propyl, diethylene glycol, and triethylene glycol. The elongation of the prosthetic group by only one methylene group (propyl vs ethyl) resulted in a tracer, [18F]**4**, that was significantly more stable in mouse, rat, and human serum than the prototype compound. This compound also showed improved cardiac imaging characteristics compared to [18F]**3**. Similarly, the myocardial uptake of [18F]**5**, the diethylene glycol ester, was significantly increased while the clearance of nontarget tissues (e.g., liver, blood, lung) was also improved. Unfortunately, however, the triethylene glycol ester showed no additional improvement, and current efforts are therefore being directed toward further studies on [18F]**5**.

In combination, these results confirm our original premise: 18F-labeled rhodamines are promising candidates for continued evaluation as PET myocardial perfusion tracers. They also suggest that further examination of the role of prosthetic groups in the biodistribution and in vivo stability of 18F-labeled compounds is warranted.

EXPERIMENTAL SECTION

General. Rhodamine B lactone (>97%) was purchased from MP Biomedical (Solon, OH). Rhodamine B chloride salt was obtained from Sigma-Aldrich (St. Louis, MO). Propane-1,3-diol ditosylate was purchased from Acros Organics (Fair Lawn, NJ), and diethylene glycol ditosylate and triethylene glycol ditosylate were purchased from TCI (Waltham, MA). For the radiosynthesis, extra dry reagent grade acetonitrile (Thermo Scientific) and Kryptofix (K2.2.2) (98%) (Sigma-Aldrich) were used. Potassium carbonate (99.97%) was purchased from Alfa Aesar (Ward Hill, MA). Other solvents and reagents were of the highest grade commercially available and used without further purification. Tetrabutylammonium fluoride (1 M in THF) was purchased from Sigma-Aldrich. 3-Fluoropropanol was obtained from Oakwood Products, Inc. (West Columbia, SC). The purity of the nonradioactive (19F) reference compounds was ≥95% as determined by analytical HPLC and NMR. Thin-layer chromatography (TLC) was performed using silica gel IB-F coated plastic sheets from J. T. Baker (Phillipsburg, NJ). Nuclear magnetic resonance spectra were obtained using a Varian 600 MHz VNMRS system or a 400 MHz Varian 400-MR system (Palo Alto, CA). Chemical shifts are given as parts per million (ppm) and are reported relative to tetramethylsilane. Coupling constants are reported in hertz (Hz). The multiplicity of the NMR signals is described as follows: s = singlet, d = duplet, t = triplet, q = quartet, m = multiplet. High-resolution mass spectra (ESI-MS mode) were obtained at the University of Illinois Mass Spectrometry Facility using a Micromass 70-VSE spectrometer. Fluorine-18 (as F⁻ in water) was purchased from Cardinal Healthcare (Woburn, MA) and Brigham and Women's Hospital (Boston, MA).

Purification and Quality Control. Analytical HPLC was carried out using a Hitachi 7000 system including an L-7455 diode array detector, an L-7100 pump, and a D-7000 interface. The radiometric HPLC detector comprised Canberra nuclear instrumentation modules and was optimized for 511 keV photons. An LaChrom PuroSphere

Star C18e column (4 mm × 30 mm, 3 μm) was used for analytical measurements. The solvent system consisted of 0.1% trifluoroacetic acid (TFA) in water (solvent A) and 0.1% TFA in acetonitrile (solvent B) at a flow rate of 1 mL/min at room temperature. The solvent gradient was 0−15 min (30−70% B), 15−25 min (70% B). The serum stability graph was created from the raw HPLC data using GraphPad Prism (GraphPad Software, La Jolla, CA). For semipreparative HPLC, an ISCO system comprising an ISCO V4 variable wavelength UV−visible detector (operated at λ = 550 nm), ISCO 2300 HPLC pumps, a radiometric γ detector similar to that described above, and a Grace Apollo C18 column (10 mm × 250 mm, 5 μm) was used. Semipreparative HPLC method A (isocratic) consisted of the following: 40% solvent A, 60% solvent B; flow rate, 5 mL/min; room temperature. Semipreparative HPLC method B (gradient) consisted of the following: 0−10 min (40% B); 10−30 min (40−50% B); 30−35 min (50−100% B); 35−40 min (100% B); flow rate, 5 mL/min; room temperature. Radiofluorination yields were determined by thin-layer chromatography using silica gel plates and chloroform/methanol (8:1 v/v) as the solvent. After development, the TLC strips were cut into 1 cm pieces and counted with a Packard Cobra γ counter.

Synthesis of Reference Compounds. 2-(2-Fluoroethoxy)-ethyl Tosylate (1). Diethylene glycol ditosylate (500 mg, 1.21 mmol) was dissolved in 5 mL of anhydrous THF under argon. The solution was heated to 80 °C followed by the addition of 2.42 mL of 1 M TBAF in THF. Product formation was monitored by TLC using a mixture of ethyl acetate/hexane 1:1 (v/v). After 15 min of heating, the starting material was fully converted as confirmed by TLC, and the reaction was stopped by cooling in an ice bath. After rotary evaporation to remove solvent and the difluorodiethylene glycol formed during the reaction, the remaining pale-yellow oil was purified by silica gel column chromatography using ethyl acetate/hexane 1:1 (v/v) as the eluent. Fractions containing the product were combined and the solvent was removed by rotary evaporation to provide **1** as a colorless oil. Yield: 262 mg (83%). ^{1}H NMR (CDCl$_3$, 400 MHz): δ 7.80 (2H, d, J = 8.26), 7.35 (2H, d, J = 8.20), 4.48 (dt, 2H, J_1 = 48, J_2 = 4.20), 4.18 (t, 2H, J = 4.80), 3.71 (m, 3H), 3.63 (m, 1H), 2.45 (s, 3H).

2-(2-(2-Fluoroethoxy)ethoxy)ethyl Tosylate (2). Compound **2** was prepared and purified by a procedure similar to that described for **1** except that triethylene glycol ditosylate was used as the starting material instead of diethylene glycol ditosylate. Yield: 249 mg (74%). ^{1}H NMR (CDCl$_3$, 400 MHz): δ 7.80 (2H, d, J = 8.31), 7.35 (2H, d, J = 8.42), 4.54 (dt, 2H, J_1 = 48, J_2 = 4.20), 4.17 (m, 2H), 3.75 (m, 1H), 3.71−3.65 (m, 3H), 3.61 (m, 4H), 2.45 (s, 3H) ppm.

Rhodamine B 3-Fluoropropyl Ester (4). Rhodamine B (chloride salt, 200 mg, 0.42 mmol), NHS (53 mg, 0.46 mmol), DCC (95 mg, 0.46 mmol), and DIPEA (80 μL, 0.46 mmol) were mixed in 10 mL of anhydrous acetonitrile under an inert atmosphere (argon). After 3 h, 32 mg (0.42 mmol) of 3-fluoropropanol was added and stirring was continued overnight. The solvent was removed by rotary evaporation under reduced pressure, and the dark purple residue was prepurified by silica gel flash chromatography using ethyl acetate/acetone 1:2 (v/v). The crude product was eluted with methanol. The purity of the crude product was >95% according to NMR characterization. In order to obtain a high purity reference material, a small fraction of the crude product was further purified by semipreparative HPLC using the same conditions as for the radioactive compound (method A). Yield (crude product): 165 mg (73%). ^{1}H NMR (CDCl$_3$, 600 MHz): δ 8.29 (d, 1H, J = 7.71), 7.81 (t, 1H, J = 7.50), 7.75 (t, 1H, J = 7.58), 7.33 (d, 1H, J = 7.25), 7.07 (m, 2H), 6.81 (m, 4H), 4.36 (dt, 2H, J_1 = 47, J_2 = 5.73), 4.17 (t, 2H, J = 6.18), 3.60 (q, 8H, J = 6.95, 14.03), 1.88 (m, 2H), 1.32 (t, 12H, J = 6.89) ppm. ^{19}F NMR (CDCl$_3$, 600 MHz): −75.8 ppm. HRMS m/z (%): calcd for C$_{31}$H$_{36}$FN$_2$O$_3^+$ [M$^+$] 503.2710, found 503.2704 (100%).

Rhodamine B 2-(2-Fluoroethoxy)ethyl Ester (5). Rhodamine B lactone (354 mg, 0.80 mmol) was dissolved in 10 mL of acetonitrile, and the solution was heated to 80 °C before adding 262 mg (1.00 mmol) of **1** dissolved in 2 mL of acetonitrile and 0.5 mL (2.94 mmol) of DIPEA. The mixture was refluxed for 16 h, allowed to cool to room temperature, and evaporated to dryness. HPLC analysis revealed

incomplete conversion, and thus, the crude product was prepurified by silica gel flash chromatography using the same conditions as described for **4**. At this point, the purity of the product was >95% (by NMR). In order to obtain a high purity reference material, a small fraction of the crude product was further purified by semipreparative HPLC using the same conditions as for the radioactive compound (HPLC method B). Yield (crude): 132 mg (26%). ^{1}H NMR (CDCl$_3$, 400 MHz): δ 8.33 (dd, 1H, J = 1.14, 7.75), 7.82−7.72 (m, 2H), 7.31 (dd, 1H, J = 0.95, 7.42), 7.07 (d, 2H, J = 9.14), 6.84−6.80 (m, 4H), 4.45 (dt, 2H, J_1 = 47, J_2 = 3.8), 4.39 (m, 1H), 4.17 (m, 2H), 3.64−3.51 (m, 12H), 1.32 (t, 12H, J = 7.11). ^{19}F NMR (CDCl$_3$, 600 MHz): −75.6 ppm. HRMS m/z (%): calcd for C$_{32}$H$_{38}$FN$_2$O$_4^+$ [M$^+$] 533.2816, found 533.2808 (100%).

Rhodamine B 2-(2-(2-Fluoroethoxy)ethoxy)ethyl Ester (6). Compound **6** was prepared and purified by a procedure similar to that described for compound **5** except that **2** was used instead of compound **1**. HPLC analysis revealed incomplete conversion, and thus, the crude product was prepurified by silica gel flash chromatography using the same conditions as described for **4**. The purity of the product was >95% (by NMR). In order to obtain a high purity reference material, a small fraction of the crude product was further purified by semipreparative HPLC using the same conditions as for the radioactive compound (HPLC method B). Yield (crude): 29%. ^{1}H NMR (CDCl$_3$, 400 MHz): δ 8.34 (dd, 1H, J = 0.92, 7.75), 7.81−7.72 (m, 2H), 7.30 (dd, 1H, J = 0.77, 7.37), 7.06 (d, 2H, J = 9.79), 6.80 (m, 4H), 4.53 (dt, 2H, J_1 = 48, J_2 = 4.1), 4.17 (m, 2H), 3.74 (m, 1H), 3.66 (m, 1H), 3.62−3.53 (m, 14H), 1.32 (t, 12H, J = 7.11). ^{19}F NMR (CDCl$_3$, 600 MHz): −75.6 ppm. HRMS m/z (%): calcd for C$_{34}$H$_{42}$FN$_2$O$_5^+$ [M$^+$] 577.3078, found 577.3073 (100%).

Radiosyntheses of ^{18}F-Labeled Rhodamines. The rhodamine B esters [^{18}F]**4**, [^{18}F]**5**, and [^{18}F]**6** were prepared by a one-pot two-step procedure as previously described for [^{18}F]**3**.[31,32] Briefly, after addition of Kryptofix and K$_2$CO$_3$ to an aqueous [^{18}F]fluoride solution, the mixture was azeotropically dried in a Pierce vial using acetonitrile. Propane-1,3-diol ditosylate, diethylene glycol ditosylate, or triethylene glycol ditosylate in 0.5 mL of anhydrous acetonitrile was added to the dried residue, and the mixture was heated at 90 °C for 10 min in a sealed Pierce vial. After rapid cooling of the mixture to room temperature, a solution of rhodamine B lactone in 0.8 mL of anhydrous acetonitrile and DIPEA (3−5 drops) were added into the vial. Further heating at 160 °C for 30 min using a 30G ventilation needle gave the crude ^{18}F-labeled rhodamine, which was purified by semipreparative HPLC. Method A was used to purify [^{18}F]**4** (t_R = 22.5 min), and method B was used to purify [^{18}F]**5** (t_R = 20.5 min) and [^{18}F]**6** (t_R = 21.5 min). HPLC fractions containing the radioactive product were combined and dried under a stream of nitrogen at 65 °C. The radioactive product was then redissolved in 10% EtOH/PBS for the serum stability studies, 10% EtOH/water for the partition coefficient measurements, or 10% EtOH/saline for animal experiments. The integrity and purity of the radioactive product were confirmed by analytical HPLC. The dry down process did not affect the purity of the compounds.

Serum Stability Studies. For each experiment, 3.7−5.6 MBq (100−150 μCi) [^{18}F]**4**, [^{18}F]**5**, or [^{18}F]**6** in 20 μL of 10% EtOH/PBS was added to 200 μL of serum in a 1.5 mL Eppendorf tube, which was equilibrated at 37 °C in a water bath prior to the addition. The tubes were shaken and incubated at 37 °C. At selected time points (15, 30, 60, and 120 min), 50 μL aliquots were taken from the serum solution and 200 μL of cold (4 °C) absolute EtOH was added. The samples were stored on ice for 5 min before filtering using Eppendorf centrifuge filters (molecular weight cutoff of 30 kDa) at 13 200 rpm for 5 min at 4 °C. Cold water (200 μL) was added to the filtrate and an aliquot analyzed by HPLC. For the control, an aliquot from the 10% EtOH/PBS stock solution was taken, diluted with water and its purity confirmed by HPLC. The percentage of intact ^{18}F-labeled rhodamine ester was calculated from the chromatograms. All experiments were performed on three separate batches of compound, and three samples were obtained at each time point for each batch of compound.

Partition Coefficient Measurements. For each determination, 3.7−5.6 MBq (100−150 μCi) of [^{18}F]**4**, [^{18}F]**5**, or [^{18}F]**6** in 20 μL

10% EtOH/water was added to a mixture of 480 μL of water and 500 μL of octanol in 1.5 mL Eppendorf tubes. Samples were vortexed for 1 min and then centrifuged at 13 200 rpm for 5 min. From each sample, three 100 μL samples of both the water and the organic layer were transferred into plastic tubes, and the samples were counted with a Packard Cobra γ counter. Experiments were performed in triplicate.

Small-Animal PET Imaging Studies. All in vivo experiments (PET imaging and biodistribution) with [18F]4, [18F]5, and [18F]6 were performed in rats because of the higher in vivo stability of the previously reported compound [18F]3 in rats compared to mice. Animal studies were carried out under a protocol approved by the Children's Hospital Boston Institutional Animal Care and Use Committee. For animal studies, the HPLC-purified 18F-labeled rhodamine esters [18F]4, [18F]5, and [18F]6 were redissolved in 10% EtOH/saline. Before injection, the solution was filtered by centrifugation through a sterilized Eppendorf filter tube (0.2 μm). For PET imaging studies, a group of at least five animals were scanned. Animals were injected with 100 μL of [18F]4, [18F]5, or [18F]6 (3.7−5.6 MBq, 100−150 μCi) and anesthetized with isoflurane (2−4% in air). Data acquisition was initiated as quickly as possible after injection of the tracer. Imaging was performed using a Siemens Focus 120 microPET scanner. Data were acquired for 60 min in list mode and reconstructed into either a single 60 min image or six 10 min frames. For reconstruction, the 3D PET data were rebinned into 2D sinograms and reconstructed using the 2D ordered subset expectation maximization (2D OSEM) iterative algorithm to generate an image with a volume of $128 \times 128 \times 95$ voxels ($0.866 \times 0.866 \times 0.796$ mm^3). Image analysis was performed using the ASIPro software package (Siemens Medical Solutions). Time−activity curves (TACs) were constructed by manually drawing regions of interest (ROI) within the left ventricular myocardium and the chest and medially in the liver. All ROIs were then copied on each of the frames, and time−activity curves of mean pixel values within the ROI were generated.

Biodistribution Studies. For each compound, a total of five animals were injected with 1.1−2.2 MBq (30−60 μCi) of the 18F-labeled rhodamine in 100 μL of 10% EtOH/saline via the tail vein. At 60 min pi, animals were sacrificed by CO_2 asphyxia and weighed. Selected tissues were then excised, weighed, and assayed for 18F. The percent injected dose per gram (%ID/g) for each tissue was calculated by comparison of the tissue counts to a standard sample prepared from the injectate.

Data Analysis. Statistical analysis was performed by unpaired two-tailed t test using Prism software (GraphPad Software Inc.).

■ ASSOCIATED CONTENT

Ⓢ Supporting Information

MS (ESI+), ^{1}H NMR, and ^{19}F NMR spectra of the nonradioactive reference compounds; HPLC profiles of the nonradioactive and 18F-labeled compounds; PET images of [18F]5 and [18F]6 in the mouse; data of the serum stability studies; maximum intensity projection (MIP) of [18F]5. This material is available free of charge via the Internet at http://pubs.acs.org.

■ AUTHOR INFORMATION

Corresponding Author

*Phone: (617) 355-7539. Fax: (617) 730-0619. E-mail: alan.packard@childrens.harvard.edu.

Present Address

§Department of Nuclear Medicine, University Hospital Freiburg, 79106 Freiburg, Germany.

Notes

The authors declare no competing financial interest.

■ ABBREVIATIONS USED

PET, positron emission tomography; SPECT, single photon emission computed tomography; MPI, myocardial perfusion imaging; HPLC, high performance liquid chromatography; TLC, thin layer chromatography; ID, injected dose; ESI, electrospray ionization; TBAF, tetrabutylammonium fluoride; DIPEA, diisopropylethylamine; PBS, phosphate buffered saline; FDG, fluorodeoxyglucose

■ REFERENCES

(1) Bengel, F. M.; Higuchi, T.; Javadi, M. S.; Lautamaki, R. Cardiac positron emission tomography. *J. Am. Coll. Cardiol.* **2009**, *54*, 1−15.

(2) Machac, J. Cardiac positron emission tomography imaging. *Semin. Nucl. Med.* **2005**, *35*, 17−36.

(3) Higuchi, T.; Bengel, F. M. Cardiovascular nuclear imaging: from perfusion to molecular function: non-invasive imaging. *Heart* **2008**, *94*, 809−816.

(4) Beller, G. A.; Watson, D. D. A welcomed new myocardial perfusion imaging agent for positron emission tomography. *Circulation* **2009**, *119*, 2299−2301.

(5) Hansen, C. L.; Goldstein, R. A.; Akinboboye, O. O.; Berman, D. S.; Botvinick, E. H.; Churchwell, K. B.; Cooke, C. D.; Corbett, J. R.; Cullom, S. J.; Dahlberg, S. T.; Druz, R. S.; Ficaro, E. P.; Galt, J. R.; Garg, R. K.; Germano, G.; Heller, G. V.; Henzlova, M. J.; Hyun, M. C.; Johnson, L. L.; Mann, A.; McCallister, B. D., Jr.; Quaife, R. A.; Ruddy, T. D.; Sundaram, S. N.; Taillefer, R.; Ward, R. P.; Mahmarian, J. J. Myocardial perfusion and function: single photon emission computed tomography. *J. Nucl. Cardiol.* **2007**, *14*, e39−60.

(6) Woo, J.; Tamarappoo, B.; Dey, D.; Nakazato, R.; Le Meunier, L.; Ramesh, A.; Lazewatsky, J.; Germano, G.; Berman, D. S.; Slomka, P. J. Automatic 3D registration of dynamic stress and rest (82)Rb and flurpiridaz F 18 myocardial perfusion PET data for patient motion detection and correction. *Med. Phys.* **2011**, *38*, 6313−6326.

(7) Lazewatsky, J.; Maddahi, J.; Berman, D.; Bhat, G.; Sinha, S.; Devine, M.; Case, J.; Ehlgen, A. Development of a method for the determination of dose ratio and minimum inter-injection interval for a one-day rest-stress protocol with BMS747158 PET myocardial perfusion agent. *J Nucl. Med. Meet. Abstr.* **2010**, *51*, 600.

(8) Studenov, A. R.; Berridge, M. S. Synthesis and properties of 18F-labeled potential myocardial blood flow tracers. *Nucl. Med. Biol.* **2001**, *28*, 683−693.

(9) Ravert, H. T.; Madar, I.; Dannals, R. F. Radiosynthesis of 3-[18F]fluoropropyl and 4-[18F]fluorobenzyl triarylphosphonium ions. *J. Labelled Compd. Radiopharm.* **2004**, *47*, 469−476.

(10) Madar, I.; Ravert, H. T.; Du, Y.; Hilton, J.; Volokh, L.; Dannals, R. F.; Frost, J. J.; Hare, J. M. Characterization of uptake of the new PET imaging compound 18F-fluorobenzyl triphenyl phosphonium in dog myocardium. *J. Nucl. Med.* **2006**, *47*, 1359−1366.

(11) Madar, I.; Ravert, H.; Dipaula, A.; Du, Y.; Dannals, R. F.; Becker, L. Assessment of severity of coronary artery stenosis in a canine model using the PET agent 18F-fluorobenzyl triphenyl phosphonium: comparison with 99mTc-tetrofosmin. *J. Nucl. Med.* **2007**, *48*, 1021−1030.

(12) Shoup, T. M.; Elmaleh, D. R.; Brownell, A. L.; Zhu, A.; Guerrero, J. L.; Fischman, A. J. Evaluation of (4-[(18)F]fluorophenyl)-triphenylphosphonium ion. A potential myocardial blood flow agent for PET. *Mol. Imaging Biol.* **2011**, *13*, 511−517.

(13) Martarello, L.; Greenamyre, J. T.; Goodman, M. M. Synthesis and evaluation of a new fluorine-18 labeled rotenoid as a potential

PET probe of mitochondrial complex I activity. *J. Labelled Compd. Radiopharm.* **1999**, *42*, 1039−1051.

(14) Marshall, R. C.; Powers-Risius, P.; Reutter, B. W.; O'Neil, J. P.; La Belle, M.; Huesman, R. H.; VanBrocklin, H. F. Kinetic analysis of ^{18}F-fluorodihydrorotenone as a deposited myocardial flow tracer: comparison to 201Tl. *J. Nucl. Med.* **2004**, *45*, 1950−1959.

(15) Yalamanchili, P.; Wexler, E.; Hayes, M.; Yu, M.; Bozek, J.; Kagan, M.; Radeke, H. S.; Azure, M.; Purohit, A.; Casebier, D. S.; Robinson, S. P. Mechanism of uptake and retention of F-18 BMS-747158-02 in cardiomyocytes: a novel PET myocardial imaging agent. *J. Nucl. Cardiol.* **2007**, *14*, 782−788.

(16) Huisman, M. C.; Higuchi, T.; Reder, S.; Nekolla, S. G.; Poethko, T.; Wester, H. J.; Ziegler, S. I.; Casebier, D. S.; Robinson, S. P.; Schwaiger, M. Initial characterization of an ^{18}F-labeled myocardial perfusion tracer. *J. Nucl. Med.* **2008**, *49*, 630−636.

(17) Purohit, A.; Radeke, H.; Azure, M.; Hanson, K.; Benetti, R.; Su, F.; Yalamanchili, P.; Yu, M.; Hayes, M.; Guaraldi, M.; Kagan, M.; Robinson, S.; Casebier, D. Synthesis and biological evaluation of pyridazinone analogues as potential cardiac positron emission tomography tracers. *J. Med. Chem.* **2008**, *51*, 2954−2970.

(18) Yu, M.; Guaraldi, M.; Kagan, M.; Mistry, M.; McDonald, J.; Bozek, J.; Yalamanchili, P.; Hayes, M.; Azure, M.; Purohit, A.; Radeke, H.; Casebier, D. S.; Robinson, S. P. Assessment of ^{18}F-labeled mitochondrial complex I inhibitors as PET myocardial perfusion imaging agents in rats, rabbits, and primates. *Eur. J. Nucl. Med. Mol. Imaging* **2009**, *36*, 63−72.

(19) Yu, M.; Bozek, J.; Guaraldi, M.; Kagan, M.; Azure, M.; Robinson, S. P. Cardiac imaging and safety evaluation of BMS747158, a novel PET myocardial perfusion imaging agent, in chronic myocardial compromised rabbits. *J. Nucl. Cardiol.* **2010**, *17*, 631−636.

(20) Mou, T.; Jing, H.; Yang, W.; Fang, W.; Peng, C.; Guo, F.; Zhang, X.; Pang, Y.; Ma, Y. Preparation and biodistribution of [18]FFP2OP as myocardial perfusion imaging agent for positron emission tomography. *Bioorg. Med. Chem.* **2010**, *18*, 1312−1320.

(21) Sherif, H. M.; Nekolla, S. G.; Saraste, A.; Reder, S.; Yu, M.; Robinson, S.; Schwaiger, M. Simplified quantification of myocardial flow reserve with flurpiridaz F 18: validation with microspheres in a pig model. *J. Nucl. Med.* **2011**, *52*, 617−624.

(22) Yu, M.; Nekolla, S. G.; Schwaiger, M.; Robinson, S. P. The next generation of cardiac positron emission tomography imaging agents: discovery of flurpiridaz F-18 for detection of coronary disease. *Semin. Nucl. Med.* **2011**, *41*, 305−313.

(23) Maddahi, J.; Czernin, J.; Lazewatsky, J.; Huang, S. C.; Dahlbom, M.; Schelbert, H.; Sparks, R.; Ehlgen, A.; Crane, P.; Zhu, Q.; Devine, M.; Phelps, M. Phase I, first-in-human study of BMS747158, a novel ^{18}F-labeled tracer for myocardial perfusion PET: dosimetry, biodistribution, safety, and imaging characteristics after a single injection at rest. *J. Nucl. Med.* **2011**, *52*, 1490−1498.

(24) Lacerda, S. H.; Abraham, B.; Stringfellow, T. C.; Indig, G. L. Photophysical, photochemical, and tumor-selectivity properties of bromine derivatives of rhodamine-123. *Photochem. Photobiol.* **2005**, *81*, 1430−1438.

(25) Reungpatthanaphong, P.; Dechsupa, S.; Meesungnoen, J.; Loetchutinat, C.; Mankhetkorn, S. Rhodamine B as a mitochondrial probe for measurement and monitoring of mitochondrial membrane potential in drug-sensitive and -resistant cells. *J. Biochem. Biophys. Methods* **2003**, *57*, 1−16.

(26) Hu, Y.; Moraes, C. T.; Savaraj, N.; Priebe, W.; Lampidis, T. J. Rho(0) tumor cells: a model for studying whether mitochondria are targets for rhodamine 123, doxorubicin, and other drugs. *Biochem. Pharmacol.* **2000**, *60*, 1897−1905.

(27) Lampidis, T. J.; Hasin, Y.; Weiss, M. J.; Chen, L. B. Selective killing of carcinoma cells "in vitro" by lipophilic−cationic compounds: a cellular basis. *Biomed. Pharmacother.* **1985**, *39*, 220−226.

(28) Rusiecka, I.; Skladanowski, A. C. Induction of the multixeno-biotic/multidrug resistance system in various cell lines in response to perfluorinated carboxylic acids. *Acta Biochim. Pol.* **2008**, *55*, 329−337.

(29) De Moerloose, B.; Van de Wiele, C.; Dhooge, C.; Philippe, J.; Speleman, F.; Benoit, Y.; Laureys, G.; Dierckx, R. A. Technetium-99m

sestamibi imaging in paediatric neuroblastoma and ganglioneuroma and its relation to P-glycoprotein. *Eur. J. Nucl. Med.* **1999**, *26*, 396−403.

(30) Vora, M. M.; Dhalla, M. In vivo studies of unlabeled and radioiodinated rhodamine-123. *Nucl. Med. Biol.* **1992**, *19*, 405−410.

(31) Heinrich, T. K.; Gottumukkala, V.; Snay, E.; Dunning, P.; Fahey, F. H.; Treves, S. T.; Packard, A. B. Synthesis of fluorine-18 labeled rhodamine B: a potential PET myocardial perfusion imaging agent. *Appl. Radiat. Isot.* **2010**, *68*, 96−100.

(32) Gottumukkala, V.; Heinrich, T. K.; Baker, A.; Dunning, P.; Fahey, F. H.; Treves, S. T.; Packard, A. B. Biodistribution and stability studies of [18]Ffluoroethylrhodamine B, a potential PET myocardial perfusion agent. *Nucl. Med. Biol.* **2010**, *37*, 365−370.

(33) Coenen, H. H. Fluorine-18 labeling methods: features and possibilities of basic reactions. *Ernst Schering Res. Found. Workshop* **2007**, *62*, 15−50.

(34) Kilbourn, M. R.; Shao, X. In *Fluorine-18 Radiopharmaceuticals*; John Wiley & Sons Ltd.: Hoboken, NJ, 2009; pp 361−388.

(35) Lasne, M.-C.; Perrio, C.; Rouden, J.; Barre, L.; Roeda, D.; Dolle, F.; Crouzel, C. Chemistry of β^+-emitting compounds based on fluorine-18. *Top. Curr. Chem.* **2002**, *222*, 201−258.

(36) Cai, L.; Lu, S.; Pike, V. W. Chemistry with [18]Ffluoride ion. *Eur. J. Org. Chem.* **2008**, 2853−2873.

(37) Henriksen, G.; Platzer, S.; Marton, J.; Hauser, A.; Berthele, A.; Schwaiger, M.; Marinelli, L.; Lavecchia, A.; Novellino, E.; Wester, H. J. Syntheses, biological evaluation, and molecular modeling of ^{18}F-labeled 4-anilidopiperidines as mu-opioid receptor imaging agents. *J. Med. Chem.* **2005**, *48*, 7720−7732.

(38) Erlandsson, M.; Karimi, F.; Lindhe, O.; Langstrom, B. (18)F-labelled metomidate analogues as adrenocortical imaging agents. *Nucl. Med. Biol.* **2009**, *36*, 435−445.

(39) Erlandsson, M.; Hall, H.; Laangstroem, B. Synthesis and in vitro evaluation of ^{18}F-labelled di- and tri(ethylene glycol) metomidate esters. *J. Labelled Compd. Radiopharm.* **2009**, *52*, 278−285.

(40) Kronauge, J. F.; Noska, M. A.; Davison, A.; Holman, B. L.; Jones, A. G. Interspecies variation in biodistribution of technetium (2-carbomethoxy-2-isocyanopropane)$^{6+}$. *J. Nucl. Med.* **1992**, *33*, 1357−1365.

(41) Zea-Ponce, Y.; Mavel, S.; Assaad, T.; Kruse, S. E.; Parsons, S. M.; Emond, P.; Chalon, S.; Giboureau, N.; Kassiou, M.; Guilloteau, D. Synthesis and in vitro evaluation of new benzovesamicol analogues as potential imaging probes for the vesicular acetylcholine transporter. *Bioorg. Med. Chem.* **2005**, *13*, 745−753.

(42) Nomura, Y.; Kubozono, T.; Hidaka, M.; Horibe, M.; Mizushima, N.; Yamamoto, N.; Takahashi, T.; Komiyama, M. Predominant role of basicity of leaving group in α-effect for nucleophilic ester cleavage. *Bioorg. Chem.* **2004**, *32*, 26−37.

(43) Mock, W. L.; Zhang, J. Z. Concerning the relative acidities of simple alcohols. *Tetrahedron Lett.* **1990**, *31*, 5687−5688.

(44) Silva, C. O.; Da, S. E. C.; Nascimento, M. A. C. Ab initio calculations of absolute pKa values in aqueous solution. Part 2. Aliphatic alcohols, thiols, and halogenated carboxylic acids. *J. Phys. Chem. A* **2000**, *104*, 2402−2409.

(45) Lopez, A. I.; Ruiz, O. P. Dimeric states of rhodamine B. *Chem. Phys. Lett.* **1982**, *87*, 556−560.

(46) Yu, M.; Guaraldi, M. T.; Mistry, M.; Kagan, M.; McDonald, J. L.; Drew, K.; Radeke, H.; Azure, M.; Purohit, A.; Casebier, D. S.; Robinson, S. P. BMS-747158-02: a novel PET myocardial perfusion imaging agent. *J. Nucl. Cardiol.* **2007**, *14*, 789−798.

(47) Kronauge, J. F.; Chiu, M. L.; Cone, J. S.; Davison, A.; Holman, B. L.; Jones, A. G.; Piwnica, W. D. Comparison of neutral and cationic myocardial perfusion agents: characteristics of accumulation in cultured cells. *Int. J. Radiat. Appl. Instrum., Part B* **1992**, *19*, 141−148.